Frequency Domain-Extended Coded Random Access Scheme with Shielding Technique for Spectrum Sharing Between 5G and Fixed Satellite Services

Tita Haryanti, *Member, IEEE,* Khoirul Anwar, *Senior Member, IEEE,* and Rina Pudji Astuti, *Member, IEEE.*

***Abstract*—This paper proposes an access scheme for spectrum sharing between the fifth telecommunication generation (5G) and Fixed Satellite Services (FSS). The proposed FDE-CRA is highly motivated by the necessity of spectrum sharing between 5G and FSS in bands of 3.4–4.2 GHz such that many interfering frequencies to the FSS can be reduced. FDE-CRA makes spectrum sharing possible by the use of multiuser detection (MUD) based on the available frequencies. We optimize degree distributions by maximizing the bandwidth efficiency and minimizing loss of random access using extrinsic information transfer (EXIT) chart. We also validate the results using practical simulations of packet loss rate (PLR) and throughput performances based on computer simulations. We found that the delay in decoding is lower when the number of frequencies (K), used in MUD, is large. In this paper, we optimizes the best K for spectrum sharing between 5G and FSS. To decrease the packets loss, shielding technique is employed in this paper. This paper evaluates five types of material shielding, (i) zinc, (ii) aluminium, (iii) aluminium mesh wire, (iv) copper, and (v) copper mesh wire in urban area, and natural shielding in sub-urban and rural areas to suppress the interference from 5G cellular to the FSS. We found that zinc material is optimal to prevent 5G signals harmful to the FSS systems.**

***Keywords*—Coded Random Access, 5G, Fixed Satellite Services, Non-Orthogonal Multiple Access.**

I. INTRODUCTION

The frequency spectrum from 3.4–4.2 GHz is the candidate spectrum that is suitable for use in 5G from various considerations [1]. However, 5G has a major problem of interference with the Fixed Satellite Services (FSS) in this band. In some countries the satellite telecommunications industry communities oppose this identification because the C-Band and Extended-C-Band frequencies are still important to support satellite telecommunications, especially in tropical regions having high rainfall.

Several techniques have been developed to reduce the interference level. Some examples are International Mobile Telecommunications (IMT) interference to Very Small Aperture Terminal (VSAT) such as separation distance [2], Low Noise Amplifier (LNA) filter installation [3], antenna position in hilly area, indoor IMT Base Transceiver Station (BTS) [2], and [4] shielding technique.

Mitigation to interferences between IMT-Advanced and FSS have been presented in [5], where material-based shielding has been used. An analytic model has been developed based on the deterministic analysis of the propagation model. The material for shielding to be analyze was only zinc with 0.1 mm thickness providing high attenuation around 20 dB better compared to other materials.

Other techniques for reducing coexistence interference between IMT-Advanced and Fixed Wireless Access (FWA) has been carried out in [6]. The authors [6] examined adjacent channel interference ratios using Adjacent Channel Interference Ratio (ACIR) applied in the band 3.4–4.2 GHz to extract additional isolation needed to protect adjacent channel interference.

The authors in [7] developed Coded Random Access (CRA) as multiple access scheme for ultra-dense networks using repetition codes, which is expected to serve millions of nodes, including humans and machines simultaneously. The proposed technique can prioritize humans over the machines for future wireless Internet-of-Things (IoT) networks. The results confirm that packet-loss-rate (PLR) and throughput of humans communications exceed that of the machines. CRA does not avoid the interference, on the contrary utilizes the interference to increase the multiple access capability.

The authors in [8] developed CRA as a multiple access scheme, which is fundamental for super-dense networks. Computer simulations are carried out for the CRA scheme under Binary Erasure Channel (BEC) to model the transmission of packets in the wireless networks. The study found that a simple optimal degree distribution is effective for human groups and machines accessing the same networks. This result is useful for future applications of super dense IoT networks.

To increase the throughput for networks with star topology the author in [9] proposed a multiuser detection (MUD) of capability (K) for multiway relay systems. The technique is further extended in [10] by exploiting the direct links. The results confirmed that several Q relays and direct links both help on (i) the increase in throughput significantly and (ii) exploits the diversity of networks, which is indispensable for the future of a dense network of wireless. However, 5G consider simple networks, where multiway relay is not considered yet in the current 5G standard.

In this paper, we extend CRA to enhance the performance of multiple access using MUD K to Frequency Domain-Extended CRA (FDE-CRA) [11]. The proposed FDE-CRA does not apply bit-interleaved coded modulation with iterative decoding (BICM-ID) as in [12] to minimize the computational complexity. However, in [11] we only consider additive white Gaussian noise (AWGN) channel, where in practice we need performances under Rayleigh fading channels and other prac-

tical aspects.

In this paper, we provide several contributions to overcome the problem of coexistence between cellular and satellite communications by combining and optimizing two different methods. Our contributions are summarized as follows:

(i) We propose a new multiple access scheme based on CRA, called Frequency Domain-Extended Coded Random Access (FDE-CRA), to reduce the use of required bandwidth by 5G technology, thereby reducing interference to satellite bands.

(ii) We optimize degree distributions by maximizing the bandwidth efficiency and minimizing the loss of random access using extrinsic information transfer (EXIT) chart. Based on the EXIT analysis, the optimal degree distribution polynomial is searched and kept having only 2 terms of degree for practical reason.

(iii) We provide analysis on the shielding technique to minimize the separation distance between base station (BS) and ground station (GS) such that more flexibility is obtain on the design of 5G cellular infrastructure. Furthermore, we also show the significant improvement of the shielding technique in urban, suburban, and rural.

(iv) Other potential contributions of this paper is to provide a technical recommendations for regulators, regarding the coexistence between 5G and FSS. The results of this paper are expected to help to be one of the solutions for coexistence services between 5G and FSS in some countries.

The rest of this paper is organized as follows. Section II introduces the problem, previous works on CRA, and FSS. Section III describes the system model of the considered 5G multiple access scheme and FSS on spectrum sharing, degree distributions used in FDE-CRA, and testing scenarios. Section IV evaluates EXIT chart of FDE-CRA based on the proposed optimal degree distribution as the theoretical performance baseline, to be confirmed using a series of computer simulations. We also evaluate the performance of FDE-CRA through PLR, throughput and time consumption for decoding. Section V analyses the results of shielding technique with artificial and natural materials. Section VI provides several technical recommendations for coexistence between 5G and FSS based on the current results. Section VII concludes this paper with some concluding remarks.

II. System Model

We describe the system model of the coexistence between 5G and FSS as shown in Fig. 1, where FSS systems is experiencing interference from the 5G base station (BS) requiring for protection. FDE-CRA is proposed as a new multiple access scheme used by 5G that can minimize the spectrum sharing with FSS in bands of 3.4–4.2 GHz. The shielding technique is added to further minimize the remaining interference from 5G BS to the FSS ground station (GS) such that the separation between 5G BS and FSS GS can also be minimized. The channels between 5G BS and FSS GS are assumed to be AWGN and frequency-flat Rayleigh fading channels, where we assume that the 5G spectrum can be sliced to be less than 1 MHz such that each packet experiences narrowband channels.

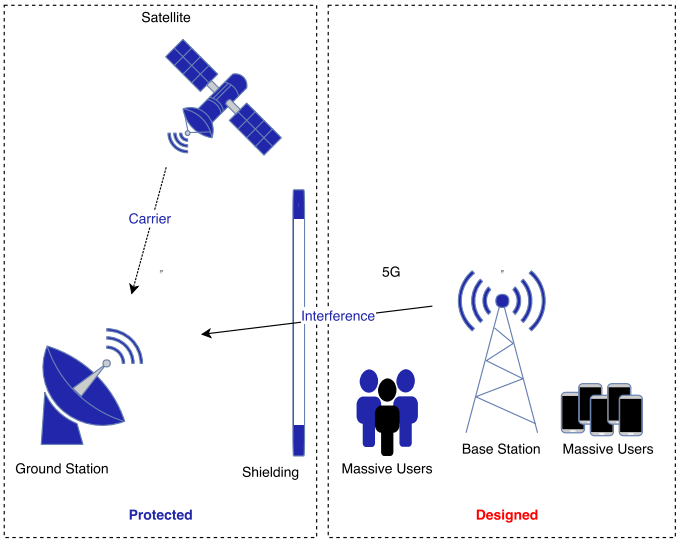

Fig. 1: System model of coexistance between 5G and FSS.

TABLE I: 5G systems parameters.

Parameter	Value
Centre frequency of operation (MHz)	3500
Channel bandwidth (MHz)	80
Base station transmitted power (W)	5
Base station antenna gain (dBi)	27
EIRP (dBm)	64
Base station antenna height (m)	6
Numerology	0

We follow the subcarrier spacing of the 5G as in [13]

$$\Delta f = 2^{\mu} \cdot 15 \text{ kHz} \quad (1)$$

and assume that the considered 5G is with numerology zero ($\mu = 0$). Other parameters are: (i) cyclic prefix is normal, (ii) minimum subcarriers is 240, (iii) minimum total bandwidth is 3.6 MHz, (iv) maximum subcarriers is 33000, and (v) maximum bandwidth is 49.5 MHz. Other parameters including FSS are summarized in Tables I and II, where the main considered environment is Indonesia because Indonesia has potential to keep the FSS systems for the whole country covering very large area and thousand of islands.

III. Proposed FDE-CRA

A. Decoding Mechanism of FDE-CRA

FDE-CRA has a similar technique to original CRA, where the massive users assumed in Fig. 1 are using non-orthogonal multiple access (NOMA) transmission with less bandwidth but exploiting large MUD capability (K).[1] Since MUD K is applied, the proposed technique has advantages of decoding

[1]In this paper, human and devices might be used interchangeably unless specified.

TABLE II: Fixed-satellite services specifications.

Parameter	Value
Antenna diameter (m)	2
EIRP (dBW)	39
Frequency f_c (GHz)	3.5
Elevation angle	74^o
Azimuth	263.7^o
Height (m)	1.8 or 5
Received noise temperature (K)	114
Bandwidth (MHz)	36
Theoretical interference level (I)	165 dBw/0.23 MHz 143 dBw/36 MHz

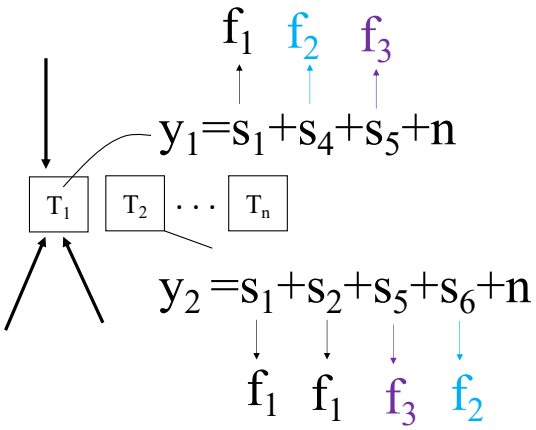

Fig. 2: The receive signal of FDE-CRA at time-slot $T_1, \cdots, T_n$, where y_1 and y_2 are composed of received signal at frequencies f_1, f_2, f_3.

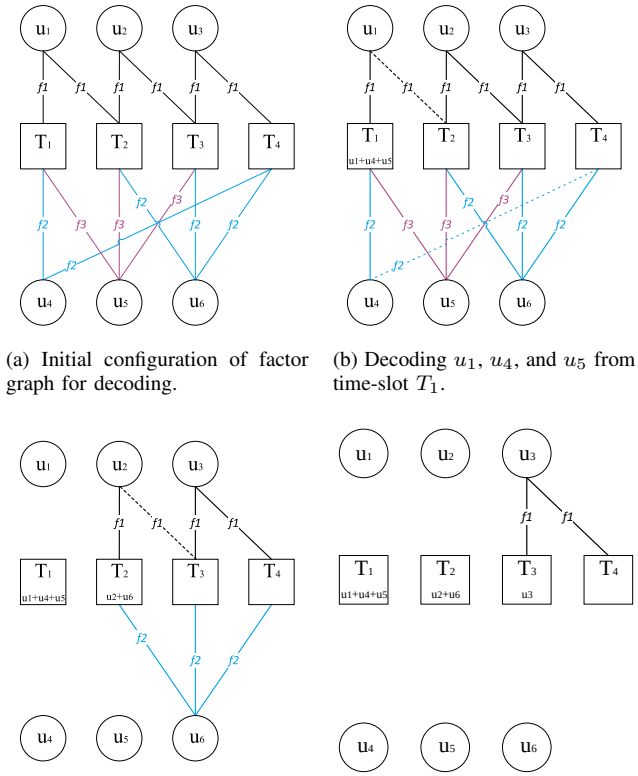

(a) Initial configuration of factor graph for decoding.

(b) Decoding u_1, u_4, and u_5 from time-slot T_1.

(c) Decoding u_2 and u_6 from time-slot T_2.

(d) All users have been successfully decoded.

Fig. 3: Decoding using FDE-CRA scheme.

K packets simultaneously at the same time-slot based on the given K available frequencies.

Fig. 2 illustrates the received signals y_1 and y_2 composed of s_1, s_2, s_4, s_5, s_6 at frequencies of f_1, f_1, f_2, f_3, and f_2, respectively. Signal s_1 represents the signal from the first user u_1, s_2 from the second user u_2, s_4 from the fourth user u_4, s_5 from the fifth user u_5, and s_6 from the sixth user u_6. The total received signal at time-slot T_n as denoted as y_n. y_1 represents the total received signal at time-slot T_1, where three different frequencies f_1, f_2, f_3 are utilized resulting in MUD with $K = 3$ since three different frequencies make simultaneous decoding possible. The signal y_1 is also corrupted by AWGN noise n. Similar way applies for y_2 at time-slot T_2, where s_1 and s_2 use f_1; s_5 uses f_3, and s_6 uses f_2. Only messages s_5 and s_6 are decodeable from T_2, however, s_1 and s_2 can be further decoded using successive interference cancellation (SIC) of FDE-CRA using decoded s_1 from T_1. The purpose of K signals using different K frequencies is to avoid collisions, such that all K users are decodeable simultaneously at the same i-th time-slot T_i, called MUD K.

Fig. 3 illustrates an example of 5G packet transmission using FDE-CRA technique expressed in a factor graph using frequency allocation of f_1, f_2, f_3 for six users. This factor graph is only viewed by BS at uplink transmission. Fig. 3(a) shows that six users are transmitting randomly at time-slots T_1, T_2, T_3, and T_4. Users u_1, u_4, u_5 can be decoded directly at time-slot T_1 because they are using f_1, f_2, f_3, respectively, as shown in Fig. 3(b). At time-slot T_2 Users u_1 and u_2 having the same frequency f_1 are accessing the same time-slot T_2. The same condition happens to Users u_4 and u_6 having the same frequency f_2 accessing the same time-slot T_4. This condition requires SIC to decode the next users using the previous decoded message. Therefore, the decoding can proceed to the next step to Users u_2 and u_6 to be decoded at time-slot T_2 as shown in Fig. 3(c). Finally the message of User u_3 can be decoded at either time-slot T_3 or T_4 as shown in Fig. 3(d).

We assume that original CRA has a large spectrumn dedicated to all users. This is because the original CRA exploit the randomness of time-slots to serve users, while the propose FDE-CRA exploit both time-slots and frequencies to serve larger number of users [11]. It is possible for FDE-CRA since FDE-CRA slice the bandwidth into K different frequencies for different users to make MUD K possible.

In this paper, we define a terminology of *bandwidth sharing efficiency* (BSE) denoted as

$$\eta = \frac{a}{b}, \tag{2}$$

where a is the bandwidth allocated for 5G, while b is the

total bandwidth of FSS systems. As an example, the total bandwidth of 100 MHz is divided into ten different frequencies $f_1, f_2, \cdots, f_{10}$ for ten users resulting in the bandwidth of $f_i = 10$ MHz, $i = 1, 2, \cdots, 10$.[2] Furthermore, we also introduce a new terminology of *clear bandwidth sharing efficiency* (C-BSE) denoting a clear bandwidth from interference coming from the 5G networks defined as

$$\bar{\eta} = 1 - \frac{a}{b} = 1 - \eta. \tag{3}$$

This C-BSE terminology is intended to evaluate how big the clear bandwidth is achieved in 5G and FSS coexistence.

We describe the BSE parameters in Fig. 4, where bandwidth of 5G FDE-CRA with several Ks are considered. Fig. 4(a) illustrates $K = 10$ and $\eta = \frac{100}{100}$. As a consequence for the bandwidth of 3.4–3.5 GHz of 100 MHz used by 5G having ten users, the $\bar{\eta}$ equals to zero.

For another case of FDE-CRA with bandwidth of 70 MHz using SIC, we have $\eta = \frac{30}{100}$, where frequency f_1 can be used up to four users as shown in Fig. 4(b). To achieve smaller η of $\eta = \frac{10}{100}$ as shown in Fig. 4(c), $K = 1$ must be used resulting in 10 MHz with $\bar{\eta}$ of 90 MHz as the clear spectrum safe for the FSS communications. These examples indicate that FDE-CRA has potential to decrease the interference of 5G to the FSS.

B. Degree Distribution for FDE-CRA

Since the proposed FDE-CRA uses random access scheme, each user randomly selects time-slots to transmit the packet to the BS. In this paper, we use $K = \{1, 2, \cdots, 10\}$ as an example.[3] To evaluate the degree distribution, we follow the terminology in [9], [10], [14]. In FDE-CRA, the degree distribution represent the distribution of packet transmitted at the selected time-slots, which is easily described using of factor graph constructed from slot node (SN) and user node (UN). The degree distribution should be optimized carefully to achieve the maximum performances of the network.

In this paper, we design the degree distribution based on repetition codes at the UN, while the distribution of the SN cannot be designed due to the nature of random transmission. According to [9] [10] [12] [15] the degree distribution of SN is following exponential distribution since each user select time-slot randomly to send the packet. The random transmission of packets at the selected time-slots by each UN. Therefore, the remaining design is only on the UN degree distribution. To make practical design, we limit the encoder of UN to repetition codes having coding rate $R = \frac{1}{16}$ resulting in maximum UN degree distribution of 16.

C. Testing Scenario

In this paper, the performances of FDE-CRA are evaluated using two testing scenarios, i.e., (i) FDE-CRA without shielding and (ii) FDE-CRA with shielding. The attenuation of standard shielding is between 0 and 40 dB depending on various types of shielding materials and environmental conditions, where the GS is located [16]. We use materials of shielding made of artificial and natural material for practical reason. According to [2] and [17], permissible interference (I) for 5G is around -117 dBm at 3500 MHz, which is also used in this paper. We consider the minimum interference power at GS of $I = -100$ dBm.

1) FDE-CRA without Shielding: The first scenario estimate the required distance to separate 5G BS and FSS GS such that $I = -100$ dBm is achievable at GS. This scenario is aiming to obtain the distance between BS and GS without shielding. To obtain the required distance, we consider pathloss of

$$P_L(\text{dB}) = 92.44 + 20\log_{10}(f) + 20\log_{10}(d). \tag{4}$$

where f is the operating frequency in GHz and d is the separation distance in km, because this pathloss can represent the condition without any obstacles.

We assume the following conditions:

1) When the GS is using off-axis antenna, the interference is calculated at the worst condition, where the interfering signal is coming from the side of $48° < \varphi \leq 180°$ at off-axis GS.
2) Interference is calculated based on 5G specification with operating frequency of 3.5 GHz.
3) Feeder loss at the transmitter and receiver is ignored.

The receiving antenna gain of off-axis antenna at GS is denoted as $G_{GS}(\varphi)$, of which the value is depending on the earth station location and the main receiving beam as [18]

$$G_{GS}(\varphi) = G_{max} - 2.5 \times 10^{-3}(\frac{D \cdot \varphi}{\lambda})^2,$$
$$0 < \varphi < \varphi_m, \tag{5}$$

where G_{max} is the maximum antenna gain (38 dBi), D is satellite diameter and λ is wavelength (m). In all scenarios carried out using the same pathloss formula and will be different when adding shield calculations

$$\begin{aligned} P_L(\text{dB}) =& 92.44 + 20\log_{10}(f) + \\ & 20\log_{10}(d) - G_{GS}. \end{aligned} \tag{6}$$

Reference [19] considers the use of clutter losses to classify the separation distance of rural, suburban, urban, and dense urban as shown in Table III, where d_k (km) is the distance from nominal clutter point to the antenna, and h_a (m) is the nominal clutter height above local ground level. Those categories show that the increase of antenna height, which is equal to the increase of clutter height, reduces the separation distance due to the different attenuation. The attenuation of each clutter is calculated as

$$\begin{aligned} A_h =& 10.25e^{-d_k}\left[1 - \tanh\left[6\left(\frac{h}{h_a}\right) - 0.625\right]\right] \\ & - 0.33, \end{aligned} \tag{7}$$

[2]This bandwidth is assumed to be small enough such that it can be considered as narrowband channel. As a consequence, in this paper, we evaluate FDE-CRA using frequency-flat Rayleigh fading channels.

[3]In practice, the parameter of K should be optimize and studied with the real-field experiments.

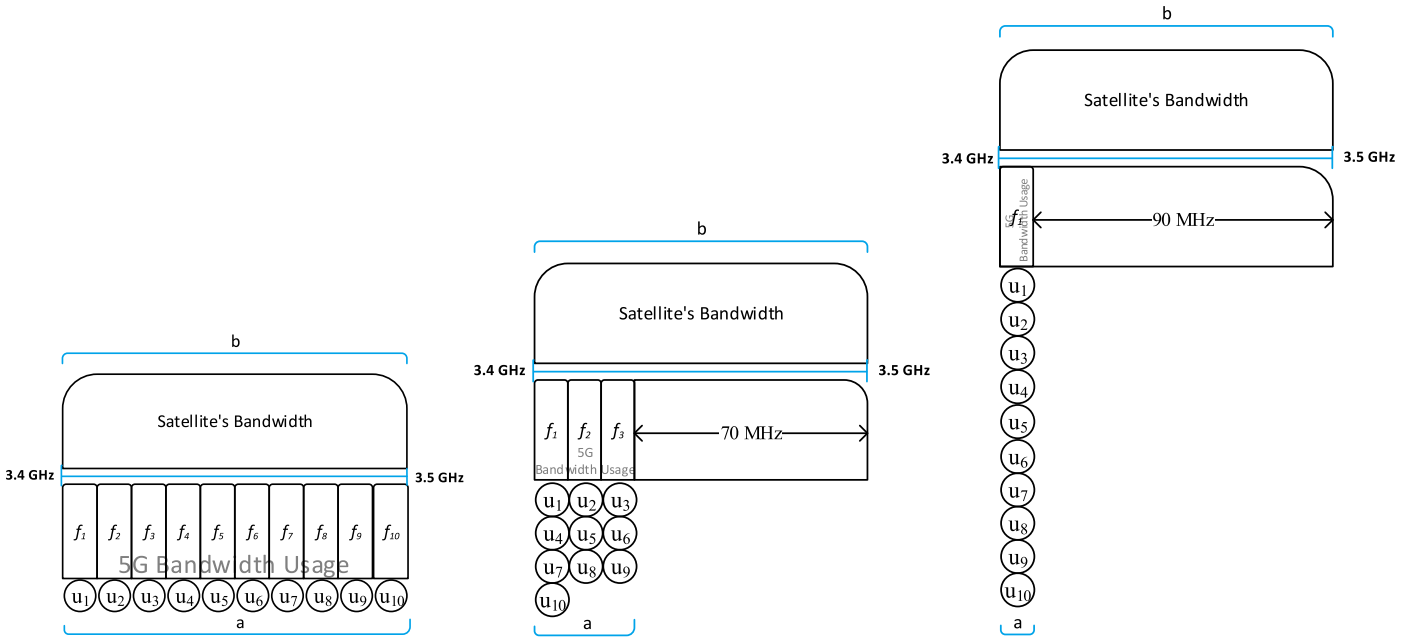

(a) $K = 10$ (b) $K = 3$ (c) $K = 1$

Fig. 4: The BSE $\eta = \frac{a}{b}$ parameters of FDE-CRA for several Ks of MUD.

TABLE III: Nominal clutter heights and distances.

Clutter Category	Clutter h_a (m)	Nominal distance d_k (km)
Rular	4	0.1
Sub-Urban	9	0.0025
Urban	20	0.02
Dense Urban	25	0.02

where h is the antenna height (m) above local ground level. Finally, by combining (6) and (7) we can obtain the total pathloss for scenario without shielding expressed as

$$P_L(\text{dB}) = 92.44 + 20\log_{10} f + 20\log_{10} d - G_{GS} + A_h. \quad (8)$$

2) Scenario with Artificial Shielding: In the non-line-of-sight (NLOS) environment, the transmit power decreases faster along the transmission line causing the performance worse, because most transmission path are blocked by objects and buildings. This paper uses the NLOS-like environment to model the interference channel from 5G to FSS. An experiment from [18] has been performed with several materials to protect the GS from BS signal, where normal shielding and mesh wire shielding are considered. Table IV [18] shows the transmission loss depending on the material shield of aluminium, aluminium mesh wire, copper, copper mesh wire, and zinc, which is considered in this paper.

In this paper, we evaluate aluminium, copper and zinc with thickness of 0.1, 0.2, and, 0.3 cm. We also evaluate the mesh wire type with spacing of 0.1, 0.2, and, 0.3 cm for both

TABLE IV: Measurements losses of signal radio paths are structured by common materials.

Material Shield (M_S)	Loss (dB)
Aluminium (0.1 cm thickness)	22.1
Aluminium mesh wire (0.2 cm wire spacing)	20.9
Copper shielding (0.1 cm thickness)	24.5
Copper mesh wire (0.2 cm thickness)	23.3
Zinc (0.1 cm thickness)	20

materials of aluminium and copper. Since shielding technique is becoming an additional loss to the pathloss, we can combine the loss of material shielding M_S to (8) resulting a total loss of

$$P_L(\text{dB}) = 92.44 + 20\log_{10} f + 20\log_{10} d - G_{GS} + A_h + M_S. \quad (9)$$

In this paper, we apply this equation (9) to model the shielding technique for urban area in determining the separation distance between BS and GS.

3) Scenario with Natural Shielding: Since the natural shielding made of tree and leaf has capabilty of attenuating the signal, it is important to exploit them in the coexistence of 5G and FSS. In this scenario, the 5G signal is obscured by the natural shielding close to the GS antenna, where the clutter loss in suburban and rural is used.

In this scenario, we use a measure of natural shielding

TABLE V: Constant values for equation (10).

Constant parameter	In leaf	Out of leaf
a	0.7	0.64
b	0.81	0.43
c	0.37	0.97
k	68.8	114.7
R_0	16.7	6.59
R_∞	8.77	3.89

TABLE VI: Degree distribution for $K = \{1, 2, \cdots, 10\}$.

Number of frequency	$\Lambda(x)$
$K = 1$	$0.50x^2 + 0.50x^4$
$K = 2$	$0.87x^2 + 0.13x^8$
$K = 3$	$0.93x^2 + 0.07x^{13}$
$K = 4$	$0.95x^2 + 0.05x^{16}$
$K = 5$	$0.97x^2 + 0.03x^{14}$
$K = 6$	$0.98x^2 + 0.02x^{15}$
$K = 7$	$0.98x^2 + 0.02x^{15}$
$K = 8$	$0.98x^2 + 0.02x^{15}$
$K = 9$	$0.98x^2 + 0.02x^{15}$
$K = 10$	$0.98x^2 + 0.02x^{15}$

attenuation following the Recommendation of ITU-R P.833-2 [20]. This model simply analyzes the attenuation by the natural shielding in the form of trees for frequency above 3 GHz. The attenuation is further modeled as a function of the thickness of the trees, where the variation of trees is ignored for practical reason.

This model is derived from a database of data measured through various frequencies. This model also take into account the geometry of the site in terms of the illumination rate of trees, defined by the width of the illumination W. The attenuation for trees depth, d (m), is

$$A_t = \frac{R_\infty}{f^a W^b} d + \frac{k}{W^c}\left(1 - \exp\left(-\frac{(R_0 - R_\infty)W^c}{k} d\right)\right), \tag{10}$$

where A_t is the trees attenuation, f is the frequency (GHz). The value of W (m) is $1 \leq W \leq 50$ with $a, b, c, k, R_0, R_\infty$ been constants given in Table V. The column of *in leaf* provide constant values for areas having natural leaves with high density, while the column of *out of leaf* provide constant values for area having sparse natural leaves. We modify (8) with natural attenuation (10), of which the total pathloss becomes

$$P_L(\text{dB}) = 92.44 + 20\log_{10} f + 20\log_{10} d - G_{GS} + A_h + A_t. \tag{11}$$

D. Optimal Degree Distribution and EXIT Chart

This paper uses similar expression as [21] and [14] for the node-perspective degree distribution of UN and SN in polynomial as

$$\Lambda(x) = \sum_d \Lambda_d x^{d-1}, \Omega(x) = \sum_h \Omega_h x^h, \tag{12}$$

respectively. Parameters d and h are the degrees of UN and SN, respectively, with Λ_d and Ω_h being the fractions or distribution of UN and SN with the corresponding degrees d and h.

In this paper, for practical reason we only use two polynomial of the degree distribution having only two fractions Λ_1, Λ_2 as

$$\Lambda(x) = \Lambda_1 x^\alpha + \Lambda_2 x^\beta. \tag{13}$$

Using this definiton, we can write the degree distributions of factor graph in Fig. 3 as $\Lambda(x) = \frac{2}{3}x^2 + \frac{1}{3}x^3$.

The degree distribution for FDE-CRA $K = \{1, 2, \cdots, 10\}$ is shown in Table VI, where $\Lambda(x) = 0.5x^2 + 0.5x^4$ means that 50% users transmit 2 packets at random time-slots and other 50% users transmit 4 packets at random time-slots during the contention period. Similar meaning applies for all Ks from $K = 2$ to $K = 10$. Since the degree distribution has two digits after the comma $V = 2$, the minimum required number of users is $M \geq 100$. In this paper, we use $M = 2000$ to satisfy the accuracy of the results in terms of PLR and throughput.

The edge-perspective degree distributions are defined as

$$\lambda(x) = \frac{\Lambda'(x)}{\Lambda'(1)}, \omega(x)\frac{\Omega'(x)}{\Omega'(1)}, \tag{14}$$

for UN and SN, respectively, where the random variable x depends on the quality of the decoded packet, which is usually expressed in erasure probabilty. We define p as the erasure probability at an edge coming out from SN expressed as

$$p = 1 - \exp\{-q\frac{G}{R}\}, \tag{15}$$

where q is the erasure probability at an edge coming out from UN, G and R is the offered traffic, defined as $G = \frac{M}{N}$, and R is the network coding rate. This paper uses multiuser detection (MUD) with available K frequencies, then we modify from the erasure probability is expressed as [12]

$$p = 1 - e^{-q\frac{G}{R}}\left(\sum_{j=0}^{K} \frac{\left(q\frac{G}{R}\right)^j}{j!}\right), \tag{16}$$

$$= \omega(q), \tag{17}$$

where additional factor of $e^{-q\frac{G}{R}}$ makes the erasure probability p smaller indicating that the successful rate of FDE-CRA is higher compared to CRA without MUD.

In this paper, we analyze the behaviour of FDE-CRA decoding using EXIT chart as in [14]. To the best our knowledge It is acceptable since the probability of erased packet can be expressed using erasure probability p as in [9] [10] [14] such that we can use binary erasure channel (BEC) channel model to simplify analysis. However, since the EXIT chart is drawn based on mutual information, we define the mutual information as

$$I = 1 - \nu, \tag{18}$$

where $\nu = \{p, q\}$.

Since the decoding is performed at the BS we plot the EXIT chart at the BS for iteration between UN and SN involving

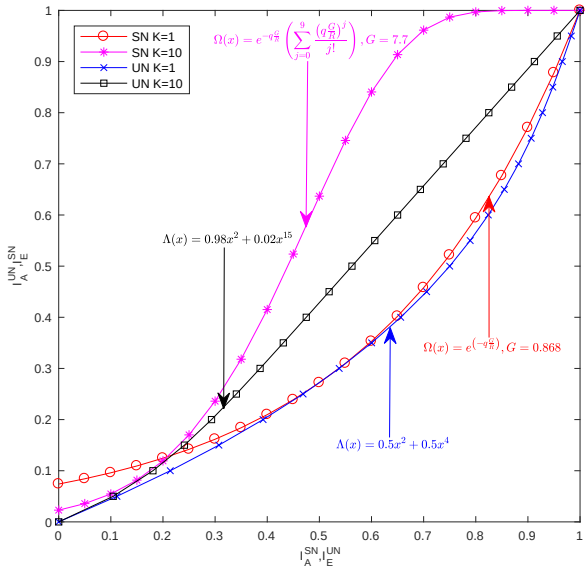

Fig. 5: EXIT chart for FDE-CRA $K = 1$ and $K = 10$.

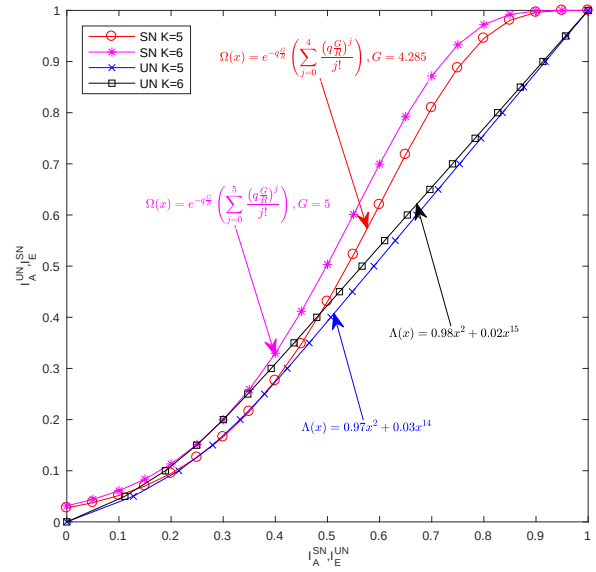

Fig. 6: EXIT chart for FDE-CRA $K = 5$ and $K = 6$.

extrinsic mutual informations for UN as

$$I_{E,UN} = 1 - \lambda(p), \quad (19)$$
$$= 1 - \lambda(1 - I_{A,UN}), \quad (20)$$

where $I_{A,UN}$ is the *a priori* mutual information at the input of UN. On the other hand, the exchanged extrinsic mutual information coming out from the SN is

$$I_{E,SN} = 1 - p, \quad (21)$$
$$= \omega(1 - q), \quad (22)$$
$$= \omega(I_{A,SN}). \quad (23)$$

In this paper, we optimize the degree distribution to satisfy

$$\begin{array}{ll} \text{maximize} & G \\ \text{subject to:} & \alpha, \beta \leq 16, \\ & \delta \leq 0.001, \\ & \Lambda_1 + \Lambda_2 = 1, \\ & V = 2, \\ & 1 \leq K \leq 10, \end{array} \quad (24)$$

where the unit of gap δ is with the same unit as the mutual information in bits. We propose optimal degree distribution as shown in Table VI as the final results of optimization.

1) EXIT chart for $K = 1$ and $K = 10$: Fig. 5 shows EXIT chart for FDE-CRA $K = 1$ and $K = 10$, where the maximum throughput for $K = 1$ is $G^* = 0.868$ packet/slot serving up to 173 users. On the other hand, the maximum throughput for $K = 10$ is $G^* = 7.7$ packet/slot serving up to 1540 users. We also confirm from this EXIT chart that there is no intersection point between UN curve and SN curve until (1,1) point indicating that successful decoding is achieved for FDE-CRA $K = 1$ and $K = 10$.

Fig. 5 confirmed that a significant difference appears on the gap of EXIT curves for $K = 1$ and $K = 10$ showing that wider gap follows the increase of higher K. It is because a component of $\sum_{j=0}^{K} \frac{(q\frac{G}{R})^j}{j!}$ in (16), which is depending on K. Based on this observation, we expect that all analyses based on $K = 1$ and $K = 10$ is enough, such that parameter setting for $K = \{1, 2, \cdots, 10\}$ is also enough.

2) EXIT chart for $K = 5$ and $K = 6$: Fig. 6 shows EXIT chart, where the maximum throughput for $K = 5$ is $G^* = 4.285$ packet/slot serving up to 857 users, while for $K = 6$ is $G^* = 5$ packet/slot serving up to 1000 users. This EXIT chart also confirms that there is no intersection point between UN curve and SN curve until (1,1) point indicating that successful decoding is also achieved for FDE-CRA $K = 5$ and $K = 6$. Similar to Fig. 5, Fig. 6 also confirms that a big difference also appears on the gap of EXIT curves for $K = 5$ and $K = 6$.

E. Packet Loss Rate (PLR) Analysis

We consider the number of frequencies $K = \{1, 2, \cdots, 10\}$ for 2000 users and 200 time-slots to evaluate the PLR performances, of which the results are shown in Fig. 7. These results indicate the ability of the proposed system to decode packets. FDE-CRA with $K = \{1, 2, \cdots 10\}$ can decode one, two, three, until ten packets, respectively. If at a single time-slot more than K packets are received, the system considers all packets at this time-slot to be stored and kept for the next decoding.

With the proposed mechanism, the loss starts at $G = 0.81$ packets/slot with PLR of 0.122 for $K = 1$, $G = 1.69$ packets/slot with PLR of 0.019 for $K = 2$, $G = 2.5$ packets/slot with PLR of 0.015 for $K = 3$, $G = 3.25$ packets/slot

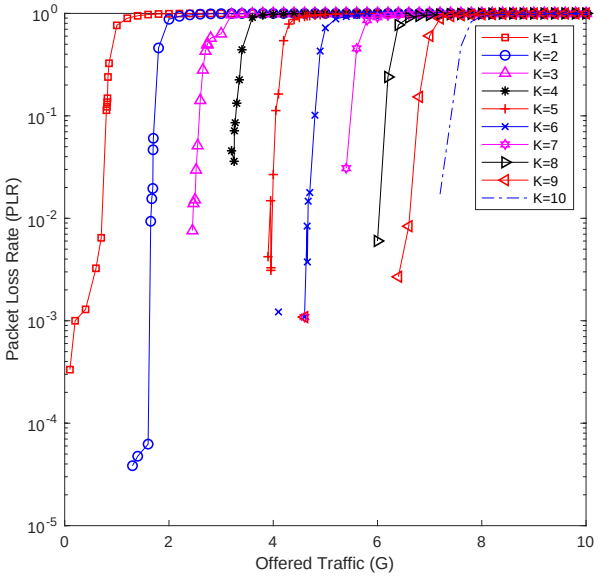

Fig. 7: PLR chart for $K = \{1, 2, \cdots, 10\}$.

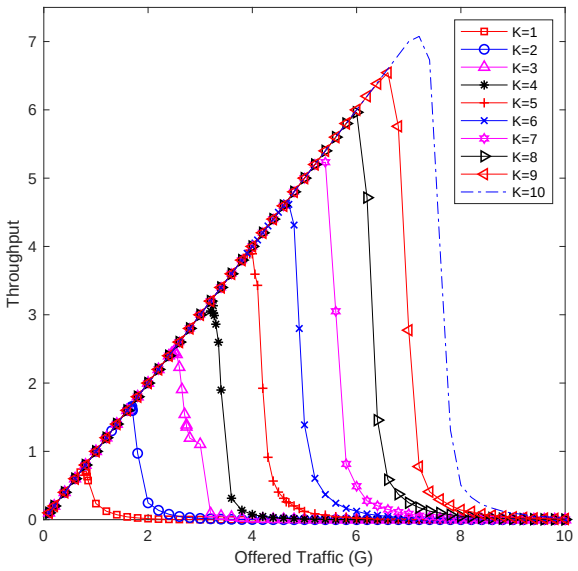

Fig. 8: Throughput chart for $K = \{1, 2, \cdots, 10\}$.

with PLR of 0.036 for $K = 4$, $G = 3.96$ packets/slot with PLR of 0.005 for $K = 5$, $G = 4.66$ packets/slot with PLR of 0.004 for $K = 6$, $G = 5.4$ packets/slot with PLR of 0.031 for $K = 7$, $G = 6$ packets/slot with PLR of 0.006 for $K = 8$, $G = 6.6$ packets/slot with PLR of 0.008 for $K = 9$, $G = 7.2$ packets/slot with PLR of 0.017 for $K = 10$.

F. Throughput Analysis

The throughput is shown in Fig. 8, where the maximum throughput is $T_{hr} = 7.07$ packets/slot achieved by $K = 10$. Other maximum throughputs are achieved at lower T_{hr} according to the corresponding K. All throughput performances are evaluated for 2000 users with 200 time-slots.

Fig. 8 with the X-axis being an offered traffic G and the Y-axis being the throughput shows that the peak throughput of FDE-CRA $K = 1$ serves $M^* = 0.71 \times 200 = 142$ users and FDE-CRA $K = 2$ serves $M^* = 1.66 \times 200 = 331$ users. Similar calculation applies for FDE-CRA $K = 3$ serving $M^* = 2.46 \times 200 = 492$ users, $K = 4$ serving $M^* = 3.13 \times 200 = 626$ users, $K = 5$ serving $M^* = 3.93 \times 200 = 787$ users, $K = 6$ serving $M^* = 4.63 \times 200 = 926$ users, $K = 7$ serving $M^* = 5.23 \times 200 = 1046$ users, $K = 8$ serving $M^* = 5.96 \times 200 = 1192$ users, $K = 9$ serving $M^* = 6.54 \times 200 = 1308$ users, and $K = 10$ serving $M^* = 7.07 \times 200 = 1414$ users. After maximum T^*_{hr} is achieved, the throughput drops because of overload since too many users are accessing the networks simultaneously.

IV. Performances Evaluation

A. Theory and Simulation Analysis

We have made an initial theory to find the maximum number of users, before simulating, it through PLR and throughput parameters to find the maximum offered traffic (G^*). The theory is done using EXIT chart, by comparing two non-intersecting graphs before reaching the x and y-axes at (1.1). Fig. 9 shows that the gap between the number of frequencies (K) and G^* increases exponentially. From these results, we found that the number of frequencies (K) may not be too large, this is because when the number of frequencies (K) is too larger, the efficiency value of the maximum offered traffic (G^*) is lower. Then, the loss of random access is higher, when the number of frequencies (K) is larger. In addition, we found that EXIT chart can be used as a prediction for the results of this research. This paper calculate the loss of random access (L) between the simulation (L_{Sim}) and the theory (L_{Theory}) expressed as

$$L_{Sim} = K - G_{sim}, \tag{25}$$

where G_{sim} is obtained from simulation of FDE-CRA, K is multiuser detection capability based on the available of frequencies. For loss of random access based on the theory, we subtract K and G^* as

$$L_{Theory} = K - G_{EXIT}, \tag{26}$$

where G_{EXIT} is obtained from EXIT chart.

In this paper, a constraint regarding the time consumption for decoding curve is added, to consider the effect of adding the number of frequencies (K) as shown in Fig. 9. Time consumption for decoding is an important concern, defined as

$$Delay = N + \frac{M_{dec}}{K}, \tag{27}$$

where N is number of time-slots and M_{dec} is decoded users.

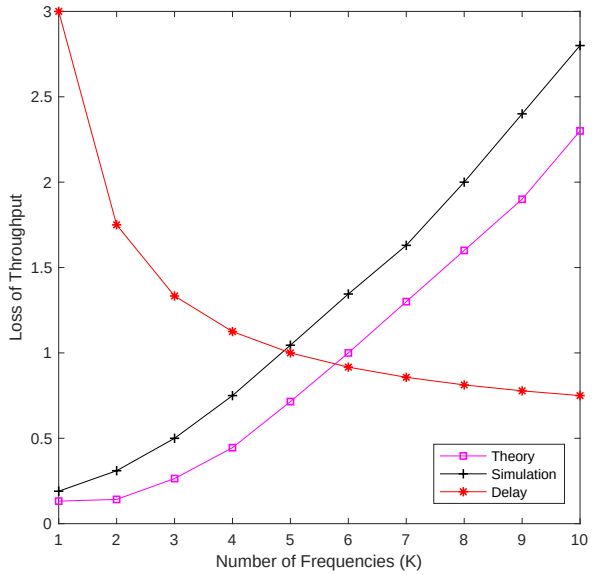

Fig. 9: Intersection among gap chart between theory, simulation and delay.

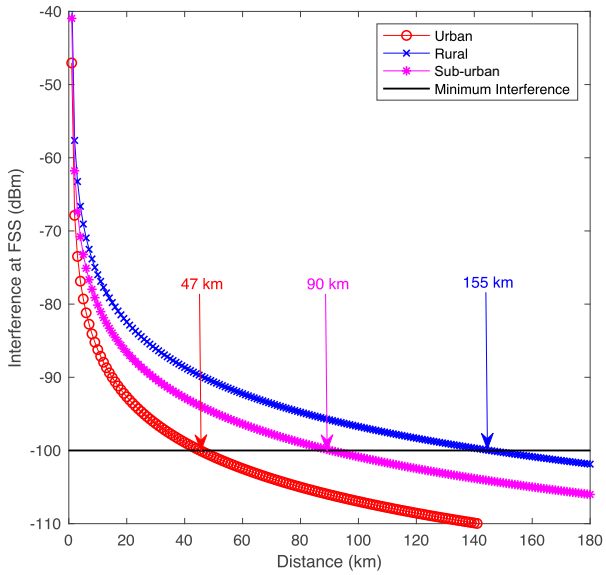

Fig. 10: Carrier to interference without shielding in urban, suburban, and rural areas.

Basically, the time consumption for decoding is lower, when the number of frequencies (K) is larger, because more users at the time-slots can be decoded at the same time simultaneously and each number of frequencies (K) is calculated as one-delay. But, the loss of random access is higher, when the number of frequencies (K) is larger. Selection with $K = 5$ is optimal among all number of frequencies (Ks) when compared to the loss of random access (L) and time consumption for decoding ($Delay$).

V. Analysis on FDE-CRA with Shielding Technique

A. The Shielding Technique

In this paper, we consider the priority of the bandwidth for 5G while the FSS is protected. In this paper, the first priority is used with the mid band frequency. In the second stage, the frequency is chosen by considering the location for implementation, which uses is bands of 3.4-4.2 GHz range. The third stage is the application of coexistence in various scenarios. In this paper, sharing bandwidth is used with the proposed FDE-CRA and shielding technique.

Interference can occur due to the use of the same frequency band and how much power is emitted by the disturber. The amount of interference is a comparison of the acceptability of the carrier that is wanted C and the carrier that interferes with I (Interference). The desired carrier is a carrier from satellite.

The calculation of the interference value between satellite communication systems and the 5G system is based on the division of three regions based on ITU recommendations, there are urban, suburban, and rural. The limit of the C/I value that is referred to is -100 dB, where the value has no signal that interferes to the FSS system.

1) Analysis without Shielding: In this paper, the calculations have been made taking into account the 5G antenna height of 20 m, GS height of 1.8 m, 3.5 GHz frequency, the gain angle (G_{GS}) of gain of 118°. This simulation using clutter loss parameters in urban, suburban, and rural areas.

Fig. 10 shows exponentially decreases of C/I. Based on the average clutter height 20 m and the average distance between clutter and GS are 0.02 km, this paper obtained the separation distance between BS and GS about 47 km. From the calculations and simulations, the separation distance with more than 47 km results interference value that can be ignored by GS. In addition, the emitted signal from BS decreases due to the reception angle of the antenna gain (G_{GS}) on the GS between 48° to 180°. Based on the average clutter height 9 m and the average distance between clutter and GS are 0.025 km, this paper obtained a separation distance between BS and GS about 90 km. From calculations and simulations, the separation distance with more than 90 km results interference value that can be ignored by GS. In addition, the emitted signal from BS decreases due to the reception angle from the antenna gain (G_{GS}) on the GS between 48° to 180°.

Based on the average clutter height 4 m and the average distance between clutter and GS are 0.1 km, this paper obtained a separation distance between BS and GS about 155 km. From calculations and simulations, the separation distance with more than 155 km results interference value that can be ignored by GS. In addition, the emitted signal from BS decreases due to the reception angle from the antenna gain (G_{GS}) on the GS $48° < \varphi < 180°$.

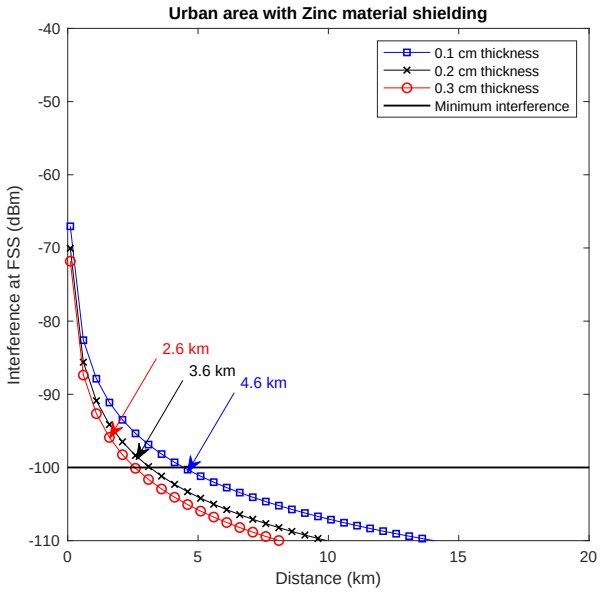

Fig. 11: Carrier to interference with material zinc shielding in urban.

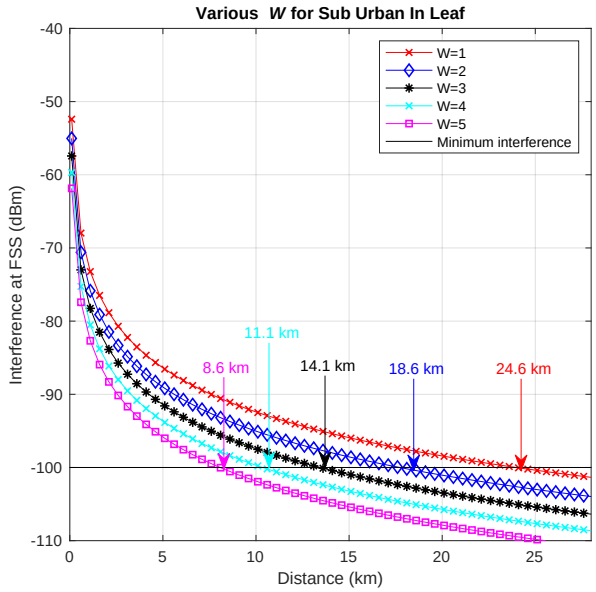

Fig. 12: Carrier to interference with natural shielding in sub-urban.

2) Analysis with Artificial Shielding: The material used is in the range of 20-24.5 dB, as shown in Table IV. In reducing a signal wave, these materials have shown a variety of weakening capabilities against radio signals. We have simulated and calculated for attenuation values using zinc, aluminium, and copper materials based on the type of modelling. There are five types of modelling, zinc, aluminium, aluminium mesh wire, copper, and copper mesh wire. We found that radio signals absorbed by materials according to the scheme block signals such as Faraday's induction law [22].

Fig. 11 clearly shows that the ability of zinc material to obtain signal attenuation is higher when a shielding technique is used compared to signal attenuation before the shielding applied. In addition, zinc also produces a closer distance between BS and GS, where the distance without shielding is 47 km, decreasing to around 2.6 km. The use of 0.3 cm thickness zinc material in urban areas is very effective because the material is available and does not disturb the surrounding environment. It can be concluded that to reduce interference between BS and GS using attenuator material zinc 20 dB, the separation distance can be reduced to 90%. We also evaluated the thickness of material zinc to improve shielding capability. The results show that thickness in 0.1 and 0.2 cm obtained separation distance around 4.6 km and 3.6 km, respectively.

3) Analysis with Natural Shielding: In this paper, we use parameters from Table V, where *in leaf* is selected. The assumption and reason for choosing *in leaf*, because Indonesia is a fertile tropical region and has relatively dense trees. However, thick trees are not too tight between each tree, so radio waves can pass through the gaps between trees. From our assumptions, we made the reference for the absorption of vegetation media and evaluating the depth of light absorption through W notation, where we changed the W value to analyze the separation distance obtained in suburban and rural areas.

We assumed that $W = 1$ is condition with low illumination width from the rare tree with few leaves. It is settle with suburban condition in rice fields, while $W = 2$ shows more trees close with each others and we assumed its condition same as plantation fields on hilly land. $W = 3$ illustrates in some leaves on a tree and it has closer among the tress like a tea fields. We assumed for $W = 4$ and $W = 5$ with same thickness but different in dense among the trees. We used $W = 4$ for rural condition that have fruit plantations like mango or avocado trees. The last is $W = 5$, where its condition perfect sense for Indonesia rural area that will be builded with 5G base station like tropical forest [20].

Fig. 12 shows the difference of separation distances based on the thickness of the leaves in the trees. We used $W = \{1, 2, 3, 4, 5\}$, where the maximum value set by ITU-T [20] is 50 (very thick and dense) for suburban area. We obtain the separation distance value if the tree area has similarities with $W = \{1, 2, 3, 4, 5\}$ are 24.6, 18.6, 14.1, 11.1 and 8.6 km, respectively. From these results it can be analyzed that the thicker the tree (in this case W), will shorten the separation distance between BS and GS.

B. FDE-CRA with Shielding Technique

To prove our proposed technique, we sent packet from user under Rayleigh fading channels using single-path or frequency-flat for narrowband systems. Wireless network conditions cause data to be vulnerable to being lost when passing a

Rayleigh fading frequency-flat channel, resulting in an error-floor, which is a condition when the error does not drop even though noise is almost zero.

Frequency-flat Rayleigh fading channel is an information channel that only contains one path and the value of the channel follows a Rayleigh distribution with probability density function (*pdf*)

$$P(\bar{\boldsymbol{z}}) = \frac{\Gamma}{\sigma^2} \exp\left(-\frac{\Gamma^2}{2\sigma^2}\right), \tag{28}$$

where σ^2 and $\frac{\Gamma^2}{2}$ are the variance of the complex signal and the bit energy received. The signal that passes through channel Frequency-flat Rayleigh fading channel is accepted by the model

$$\boldsymbol{y} = h \cdot \bar{\boldsymbol{z}} + \boldsymbol{n}, \tag{29}$$

where n is vector of additive white Gaussian noise (AWGN) and h is the value of Rayleigh fading channels, which is employed to be random channel in a block of transmission.

To simulate FDE-CRA under Rayleigh fading channel, we assume that packets is dropped or erased when the received power is lower that threshold T_h, of which the probability is [23]

$$Pr(\gamma \leq T_h) = \int_0^{T_b} Pr(\gamma) d\gamma, \tag{30}$$

where $Pr(\gamma) = \frac{1}{\Gamma} \exp(\frac{\gamma}{\Gamma})$. To simplify without removing the general nature, in this paper, we assume $\Gamma = 1$ with $T_h = 0.25$ for simulation of FDE-CRA under Rayleigh fading channel without shielding technique and $T_h = 0.15$ for simulation of FDE-CRA under Rayleigh fading channel with shielding technique. Based on (30), the probability of induced from a user using a degree h to a user using a degree $\tilde{h}$, where $0 \leq \tilde{h} \leq h$ is

$$P_{h \to \tilde{h}} = \binom{h}{h - \tilde{h}} (P_d)^{h-\tilde{h}} (1 - P_d)^{\tilde{h}}, \tag{31}$$

where $P_d = 1 - \exp(\frac{T_h}{\Gamma})$ is an edge probability from Rayleigh fading channels as written in (30). We also show example impact of Rayleigh fading channels from degree distribution $\Lambda(x) = 0.97x^2 + 0.03x^{14}$ to induced degree distribution $\Lambda'(x)$ as shown in Table VII.

We also consider one of important numerical calculation to prove that the Signal to Noise Ratio (SNR) value for noise affects the Rayleigh fading channel.

$$\text{SNR} = \frac{S}{N + I}, \tag{32}$$

where S is signal, N is noise, so we assume $S = 1$, $N = 1$ and interference is $I = 0$ for simulation of FDE-CRA under Rayleigh fading channel without shielding. The appearance of interference occurs where shielding technique is employed and $I = 1$. The SNR before employe shielding technique is bigger than after using shielding technique. From the calculation of SNR, we used T_h using without shielding technique greater than using shielding technique. Thus, we use $T_h = 0.25$ for simulation without shielding technique and $T_h = 0.15$ for simulation with shielding technique.

TABLE VII: An example of induced degree distribution from $\Lambda(x) = 0.97x^2 + 0.03x^{14}$ to $\Lambda'(x) = 0.259 + 0.259x + 0.453x^2 + 0.002x^8 + 0.006x^9 + 0.002x^{10} + 0.006x^{11} + 0.01x^{12} + 0.002x^{13} + 0.002x^{14}$.

	x^2	x^{14}	$\Lambda'(x)$
	0.97	0.03	
x^0	0.2667	0	0.258699
x^1	0.2667	0	0.258699
x^2	0.4667	0	0.452699
x^3		0	0
x^4		0	0
x^5		0	0
x^6		0	0
x^7		0	0
x^8		0.0667	0.002001
x^9		0.2	0.006
x^{10}		0.0667	0.002001
x^{11}		0.2	0.006
x^{12}		0.333	0.0099
x^{13}		0.0667	0.002001
x^{14}		0.0667	0.002001

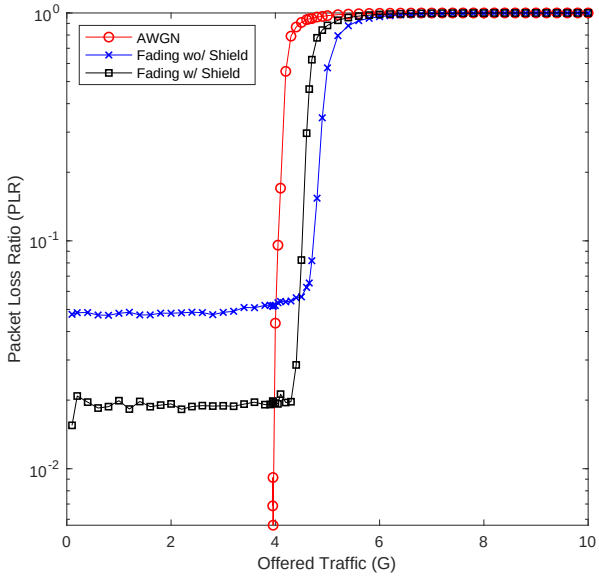

Fig. 13: FDE-CRA $K = 5$ comparison between AWGN, Rayleigh fading without shielding, and Rayleigh fading with shielding.

1) Packet Loss Rate (PLR) Analysis: Fig. 13 describes the performance of FDE-CRA $K = 5$, where the AWGN channel and Rayleigh fading channel is considered in this paper. From the simulation result, FDE-CRA shows that the packets under Rayleigh fading channel improve performance caused by failed user to send packets. FDE-CRA exploit Rayleigh fading to decrease number of degree on time-slots. Thus, if six users send packets to one time-slot, the users can not be decoded. We assume from six users, one users has poor channel ($|h|^2 < T_h$), so one user failed sent packets, but five users can be decoded

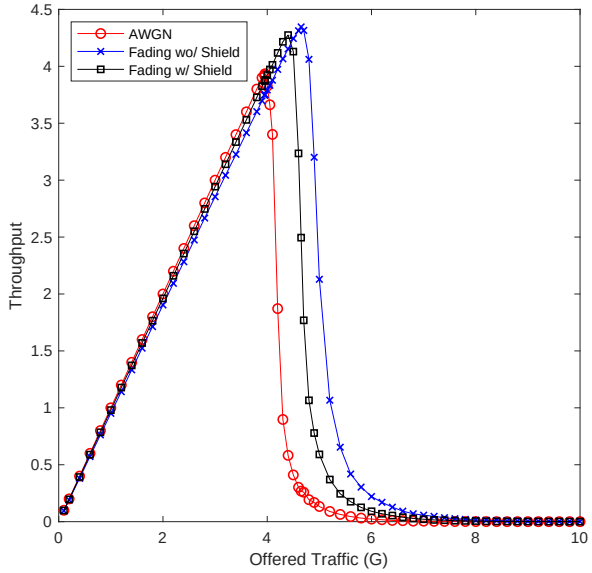

Fig. 14: Throughput performance of FDE-CRA $K = 5$ through channel AWGN, Rayleigh fading without shielding and Rayleigh fading with shielding technique

using FDE-CRA $K = 5$. By comparing when $G = 5$, where number of users is 1000, FDE-CRA under AWGN channel obtain bad performance that is 0.93 (almost asymtotic), while under Rayleigh fading channel without shielding obtain PLR 0.57. In addition, after employing a shielding technique the performance does not increased caused by interference (shielding), where PLR is 0.88. However, under AWGN channel, FDE-CRA still has best result of channel condition as shown in G between 0 and 4. FDE-CRA under AWGN channel has perfect condition to serves the packets from users, while under Rayleigh fading channel without shielding technique has a lot of packets loss due to serious error-floor.

2) Throughput Analysis: Fig. 14 illustrates throughput from the PLR performances, where packets under AWGN channel, Rayleigh fading channel without shielding and Rayleigh fading channel with shielding technique. The result shows that FDE-CRA $K = 5$ under AWGN channel can reach throughput T_{hr} up to 3.93 packets/slot at $G = 3.96$, under Rayleigh fading channel without shielding can reach throughput T_{hr} up to 4.35 packets/slot at $G = 4.65$. Because under Rayleigh fading channel without shielding, there are a number of packets that fall when passing an unstable channel model, while under AWGN channel, there is no packets that falls because the channel model is ideal. On the other hand, under Rayleigh fading channel with shielding technique can only reach maximum throughput T_{hr} of 4.27 packets/slot at $G = 4.40$. The addition of shielding technique reduces the effect of Rayleigh fading channel, so that packets can be sent, but due to more packets being sent, the decoding process is harder.

VI. Technical Recommendations

After we conducted a comprehensive paper of the issue of interference between FSS and 5G, we obtained several technical recommendations:

1) We obtained that the delay process in decoding is smaller when the number of frequencies (K) used in MUD is high. This is due to the decoding process is more efficient because many signals received at the same time slot can be decoded.
2) We found that MUD of FDE-CRA $K = 5$ is optimal with bandwidth sharing efficiency beyond 50%.
3) We recommended zinc material because it has lifespan longer than aluminium and copper.
4) We obtained for the separation distance caused by zinc decreased around 94.4% for urban area, natural shielding with $W = 5$ for suburban and rural area up to 90.4% and 90.2%, respectively.
5) We discovered that FDE-CRA $K = 5$ optimal and suitable in AWGN channel where PLR performance shows zero packet loss until $G = 4$, and FDE-CRA $K = 6$ has perfect channel until $G = 4.2$. The Rayleigh fading channel worse than AWGN channel where packets loss occur in the beginning of G. By using shielding technique, the result shows that performance for FDE-CRA increase because the shielding technique can prevent FSS from 5G interference.

VII. Conclusions

We have proposed FDE-CRA using EXIT chart to make the coexistence between 5G and FSS possible and practical, where interference is further suppressed by the material shielding. The FDE-CRA is developed based on MUD with $K = \{1, 2, \cdots, 10\}$ using available 5G spectrum such that the interference to the FSS is significantly reduced. Based on EXIT analysis, the optimal degree distribution is obtained for each MUD K with 2-term degree distributions. We have also evaluated PLR and throughput performances to prove the prediction based on EXIT chart using a series of computer simulations.

According to EXIT analysis, we found that FDE-CRA using $K = 5$ has better decoding/detection performances and smaller loss with smaller gap to the theoretical curve compared to FDE-CRA $K = 6$, where the achieved G based on EXIT chart is 4.285 for FDE-CRA $K = 5$. However, 5G with FDE-CRA $K = 6$ has better performances and serves more users with peak throughput of $G = 4.655$ packet/slot, but FDE-CRA $K = 6$ has wider interfering to the satellite band. The final results confirmed that FDE-CRA $K = 5$ is optimal in terms of time consumption for decoding (delay) and loss due to the use of random access. In addition, we have also analyzed the delay with almost 1000 users in decoding, where we found that the use of more frequencies results in shorter delay due to several users are decoded simultaneously.

Furthermore, we have also evaluated zinc material and natural shielding in urban, suburban, and rural areas. For the urban area, the separation distance is reduced to 2.6 km by the use of zinc material with a thickness of 0.3 cm. For suburban

and rural areas, natural shielding is based on the trees thickness to absorb radio waves ($W = 5$) providing a separation distance of 8.6 km and 14.6 km, respectively. We also calculated the ratio of the decrease on separation distance, before and after using shielding. The use of zinc material in urban areas reduces the distance to 94.4%, while the natural shielding for suburban is up to 90.4% and for rural is 90.2%.

We have also simulated FDE-CRA without and with shielding technique in frequency-flat Rayleigh fading channels. Performance of FDE-CRA under Rayleigh fading channel with and without shielding, shows that throughput performance under fading channel is better than under AWGN channel, because the induced degree distributions due to the broken links help the decoder performs successfully. These results confirm the contributions of FDE-CRA under Rayleigh fading serving more users in massive wireless networks.

REFERENCES

[1] M. J. Marcus, "Wrc-19 issues: A survey," *IEEE Wireless Communications*, vol. 24, no. 1, pp. 2–3, January 2017.

[2] M. Höyhtyä, "Sharing FSS satellite C-band with secondary small cells and D2D communications," in *2015 IEEE International Conference on Communication Workshop (ICCW)*. IEEE, June 2015, pp. 1606–1611.

[3] S. Jin, Y. Zhang, J. Xiao, H. Long, and N. Wang, "Analysis of adjacent channel interference between FSS system and IMT-A system," in *Microwave, Antenna, Propagation and EMC Technologies for Wireless Communications (MAPE), 2013 IEEE 5th International Symposium on*. IEEE, October 2013, pp. 49–53.

[4] L. F. Abdulrazak and A. Hameed, "Terrestrial-to-satellite interference in the C-band: Tractable calculation technique." *Journal of Theoretical & Applied Information Technology*, vol. 65, no. 3, July 2014.

[5] L. F. Abdulrazak and A. A. Oudah, "Interference mitigation technique through shielding and antenna discrimination," *International Journal of Multimedia and Ubiquitous Engineering (IJMUE)*, vol. 10, no. 3, pp. 343–352, October 2015.

[6] Z. A. Shamsan, F. Lway, and T. A. Rahman, "Co-sited and non co-sited coexistence analysis between IMT-advanced and FWA systems in adjacent frequency band," in *WSEAS International Conference. Proceedings. Mathematics and Computers in Science and Engineering*, no. 7. World Scientific and Engineering Academy and Society, May 2008.

[7] K. Niamah, I. N. A. Ramatryana, and K. Anwar, "Coded random access prioritizing human over machines for future IoT networks," in *International Conference on Telematics and Future Generation (TAFGEN)*. IEEE, July 2018.

[8] S. Larasati, I. Nyoman, A. Ramatryana, and K. Anwar, "High-rate coded random access for non-orthogonal multiple access with human priority," in *International Conference on Telematics and Future Generation (TAFGEN)*. IEEE, July 2018.

[9] K. Anwar, "Graph-based decoding for high-dense vehicular multiway multirelay networks," in *Vehicular Technology Conference (VTC Spring), 2016 IEEE 83rd*. IEEE, May 2016, pp. 1–5.

[10] K. Anwar, "High-dense multiway relay networks exploiting direct links as side information," in *2016 IEEE International Conference on Communications (ICC)*, May 2016, pp. 1–6.

[11] T. Haryanti and K. Anwar, "Frequency Domain-Extended coded random access scheme for spectrum sharing between 5G and fixed satellite services," in *2019 IEEE International Conference on Signals and Systems (ICSigSys) (ICSigSys2019)*. Bandung, Indonesia: IEEE, July 2019.

[12] A. A. Purwita and K. Anwar, "Massive multiway relay networks applying coded random access," *IEEE Transactions on Communications*, vol. 64, no. 10, pp. 4134–4146, October 2016.

[13] A. A. Zaidi, R. Baldemair, H. Tullberg, H. Bjorkegren, L. Sundstrom, J. Medbo, C. Kilinc, and I. Da Silva, "Waveform and numerology to support 5G services and requirements," *IEEE Communications Magazine*, vol. 54, no. 11, pp. 90–98, November 2016.

[14] F. M. Pasalbessy and K. Anwar, "Analysis of Internet of Things (IoT) networks using extrinsic information transfer (EXIT) chart," in *International Seminar on Intelligent Technology and Its Applications (ISITIA), Sanur, Bali*, August 2018.

[15] G. Liva, "Graph-based analysis and optimization of contention resolution diversity slotted aloha," *IEEE Transactions on Communications*, vol. 59, no. 2, pp. 477–487, February 2011.

[16] ITU-R, "Sf.1486-0:sharing methodology between fixed wireless access systems in the fixed service and very small aperture terminals in the fixed-satellite service in the 3400-3700 MHz band," May 2000.

[17] ——, "Sf.1006: Determination of the interference potential between earth stations of the fixed-satellite service and stations in the fixed service," April 1993.

[18] L. F. Abdulrazak, *Coexistence of IMT-Advanced Systems for Spectrum Sharing with Receivers in C-Band and Extended C-Band*. Springer, August 2018.

[19] P. Series, "Prediction procedure for the evaluation of interference between stations on the surface of the earth at frequencies above about 0.1 GHz," April 2013.

[20] ITU-R, "Attenuation in vegetation," January 1999.

[21] K. Anwar, B. Syihabuddin, N. M. Adriansyah *et al.*, "Coded random access with simple header detection for finite length wireless IoT networks," in *c, 2017 Eighth International Workshop on*. IEEE, September 2017, pp. 94–98.

[22] Drewniak, "Coupling through the magnetic field–faradays law," http://www.emcs.org/edu/ExperII/MagField Coupling.pdf, pp. 1–9, May 2010.

[23] K. Anwar and R. P. Astuti, "Finite-length analysis for wireless superdense networks exploiting coded random access over rayleigh fading channels," in *2016 IEEE Asia Pacific Conference on Wireless and Mobile (APWiMob)*. IEEE, 2016, pp. 7–13.

Tita Haryanti received B.E. degree in Electrical Engineering (Telecommunications) from the department of Electrical Engineering (Telecommunications), Telkom University, Bandung, Indonesia, in 2018. She is currently pursuing Master degree at Telkom University, Bandung, Indonesia. Since 2018, she has been with the Center for Advanced Wireless Technologies (AdWiTech) as a researcher.

Haryanti has presented a topic of Technologies for Coexistence between 5G and Fixed Satellite Services (FSS) at C-band for Agency for Research and Development of Human Resources at the Ministry of Communication and Information Technology, Ciputat, Jakarta and Telkom University, Bandung, on April 2018 and May 2019, respectively.

Her research interests are information and coding theory for wireless communications, digital signal processing, multiuser detection, interference mitigation and bandwidth management, spectrum analysis and spectrum efficiency for regulation and management of telecommunications.

Khoirul Anwar graduated (*cum laude*) from the department of Electrical Engineering (Telecommunications), Institut Teknologi Bandung (ITB), Bandung, Indonesia in 2000 for his Bachelor degree (S.T.). He received Master and Doctor Degrees from Graduate School of Information Science, Nara Institute of Science and Technology (NAIST), Nara, Japan, in 2005 and 2008, respectively. He received best student paper award from the IEEE Radio and Wireless Symposium (RWS'06) in 2006, California, USA, Best Paper Award of Indonesian Student Association (ISA 2007), Kyoto, Japan in 2007, Best Paper Presenter for the Advanced Technology in International conference on Sustainability for Human Security (SUSTAIN), Kyoto, October 2011, Indonesian Diaspora "Award for Innovation", Congress of Indonesian Diaspora, Los Angeles, USA, July 2012, Achmad Bakrie Award 2014, Jakarta, December 2014, and Anugerah of Internationally Recognized Contributions from the Governor of West Java, Indonesia, December 2016, National Achievement Award by UKP-PIP Pancasila, Jakarta, August 2017, Best paper of International Conference on Telematics and and Future Generation Networks (TAFGEN), July 2018.

Dr. Anwar was in University of Melbourne, Australia, in 2007, University of Oulu, Finland, in 2010, and Cranfield University, United Kingdom, in 2018, as a visiting researcher. In September 2008, he was with the School of Information Science, Japan Advanced Institute of Science and Technology (JAIST) as an assistant professor. Since September 2016 Dr. Anwar is with the school of electrical engineering, Telkom University, Bandung, Indonesia as an associate professor and the director of the Center for Advanced Wireless Technologies (AdWiTech). Dr. Anwar's technique is adopted by the international telecommunication union (ITU), ITU-R standard No. ITU-R S.2173 *"Multi-carrier-based transmission techniques"* also in ITU-R S.1878 *"Multi-carrier Based Transmission Techniques for Satellite Systems"*.

Dr. Anwar is the Chairman of Working Group (WG) Radio and Technologies of Indonesia 5G Forum (i5GF) and Vice-chairman of Asia Pacific Telecommunity Wireless Group (AWG) 2019–2022, where formerly he was the chairman of AWG WG Service and Applications (SA) since 2016. His research interests are network information theory, error correction coding, iterative decoding, coding for super-dense networks and signal processing for wireless communications. He serves as a reviewer for a number of main journals and conferences in the area of wireless communications, coding theory and signal processing. Dr. Anwar is a senior member of IEEE (Information Theory society, Communications society).

Rina Pudji Astuti graduated *(cum laude)* from the department of Electrical Engineering (Telecommunications), Institut Teknologi Sepuluh Nopember (ITS), Surabaya, Indonesia in 1987 for her Bachelor degree (Ir.). She has received Master and Doctoral degrees from department of Electrical Engineering (Telecommunications), Institut Teknologi Bandung (ITB), in 1999 and 2009, respectively.

Dr. Astuti has worked for National Aircraft Industry (IPTN), in 1987–1991, as a Telemetry Flight Test Engineer in Flight Test Center. Since September 1993, Dr. Astuti joined the school of electrical engineering, Telkom University, Bandung, Indonesia as a lecturer, Dean of School of Electrical Engineering, and currently as the Vice Rector for Research, Community Services and Student Affair of Telkom University, Bandung, Indonesia.

Dr. Astuti is the chairman of IEEE ComSoc Indonesia Chapter since 2016 and is also the Drafting Group chairman of Asia Pacific Telecommunity (APG) since 2016. Her research interests are mainly in the area of Wireless Technology, including Massive MIMO, Coded OFDM, MC-CDMA, Space Time Codes, Adaptive Transmission Scheme, Multiuser Detection, Cooperative and Coexistence Radio, Interference Mitigation and Bandwidth Management, Telecommunications Engineering and Regulation, Satellite systems, and Radio Techniques. She serves as a reviewer for conferences in the area of wireless communications, Telecommunications Engineering and Regulation.